31st Annual International Conference of the IEEE EMBS
Minneapolis, Minnesota, USA, September 2-6, 2009

Image and Signal Correlation of Electric-field Induced Charged Fibrous Viruses (fd)

K. Kang, *non-Member, IEEE*

Abstract—**The image and signal correlations are presented for understanding both collective and microscopic dynamics of filamentous bacteirophage, fd-virus suspensions. For a given low ionic strength, the electrostatic Debye screening length is few times larger than the diameter of the core of fd-virus particles; the applied electric field apparently deforms the double-layer and determines the interaction (or the motion).**

I. Introduction

THE time correlations of images (or pixels) and signals contain often important physiological characteristic changes in biological systems. Dynamics of soft tissues are hardly visualized in current medical imaging processes, except the ultrasonic method to speculate any "hardened" objects (such as cancerous tumor) inside human body. To visualize the slight increase of viscous liquids inside human body, it needs both "delicacy" and "efficiency" to capture any indication of ordering "advances" or "retards" in time. If one can develop the "electrically" responsive biochemical and biomechanical designed surfaces for mimicking the human organs or "surfaces", then the first challenge among research interests could be the characterization of the phase and their transitions. This type of realization can be probed by field-induced external fields, such as small differences of temperature and ion concentrations. Depending on the complexity of system itself, together its salinity environments, the object (or the body) may behave differently. Recently, designing artificial cells to monitor the biological ion concentration gradients [1] and induced gamma activities in human brain research [2] are interested in. ***To employ the scientific methods and data analysis to the development of the medical technology, we like to introduce our own studies of electric response of soft matter, and its resulting field-induced phase/ state transitions.***

We have chosen the charged fibrous viruses (fd) for our model system to investigate the various phases/states that are induced by an external oscillating electric field. The main reason for our observation is due to the fact of the electric double-layer polarization from diffusive ions that are surrounded with the fd-virus particles at a given ionic strength (~ 0.16 mM TRIS/HCl buffer). The Debye screening length is then typically few times larger than the core diameter of the fd-particle itself. Various phase/state transitions are observed as in the electric phase diagrams, together with the detailed characterizations and behaviors of each transition lines [3]-[5]. For low frequency, where the electric double-layer is responsive, the depolarized optical morphologies have shown various pattern formations by increasing the field amplitude, such as from nematic domains, chiral nematic ("fingerprint") texture, to the dynamical states of small nematic domains [4]. However for higher frequency (more than few kHz, depending on the fd-concentration), the only uniformly aligned phase is occurred due to no-response of the double-layer polarization [4]. ***In this paper, we discuss on high field strength for low frequency behavior; the field-induced dynamical states are distinguished as "slow" and "fast" state depending on field amplitudes. Video (or image) correlation functions are used to characterize this transitional kinetics for mesoscopic length and time scale of both dynamical states. Also signal processing is used with our homemade "vertical" small angle dynamic light scattering to speculate the microscopic dynamics of a length scale on ~ 1 μm (of the single fd-virus particle).***

II. Experimental Methods

A. In-Situ Electric Cell and Depolarized Optical Morphologies

To facilitate the optical observation with the applied electric field, we use our homemade in-situ electric cell that is shown in Fig.1 (a). Sample is loaded (~ 400 μl amount) on the bottom side of indium-tin-oxide (ITO) glasses, and then gently suppressed by upper ITO glass. Sinusoidal waveform of alternating current electric field is applied by a function generator to the right-side, where the electronic pin connection is up-side, while as the left-side is grounded. This gives not only solid electric connections to the sample, but also for easy access of mounting and combining with other experimental equipments, such as inverted microscopy, birefringence, and light scattering. For visual observations of depolarized optical morphologies, the CCD camera is connected to PC interface with time-lapse imaging software.

Typical depolarized images of chrial-nematic phase and dynamical states are shown in Fig. 2 (a), and (b),

Manuscript received April 7, 2009. This work is supported in part by the Transregio SFB 6018 "Physics of Colloidal Dispersions in External Fields" and the EU-FP7 Network "NanoDirect" grant number CP-FP-213948-2. K. Kang is with Forschungszentrum Juelich, IFF-Weiche Materie (corresponding author to phone: +49-2461-61-6089; fax: +49-2461-61-2280; e-mail: k.kang@ fz-juelich.de).

respectively. For chiral-phases, the optical pitch variation is measured on varying the field amplitude: apparent "measured" pitch as a projection component of the optical pitch decreases with increasing field amplitude.

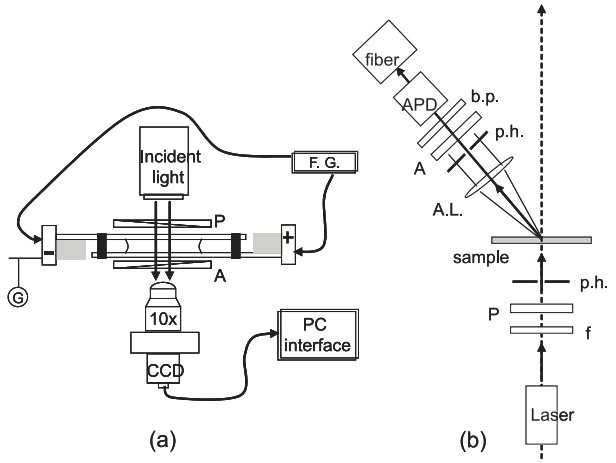

Fig. 1. Experimental schemes: (a) In-situ electric cell is loaded on top of the objective lens in inverted microscope combined with the CCD camera for video recording. F.G.: Function generator, P: polarizer, A: analyzer, G: ground. Two ITO glasses are sealed with PTFE spacer for both ends. (b) Vertical small angle dynamic light scattering setup. P: Polarizer, p.h.: pin-hole, f: filter, A.L.: achromatic lens, A: analyzer, b.p.: band pass filter, APD: avalanche photo diode. Detecting fiber is connected to the correlator in PC.

Also the broad pitch deviation at low amplitude becomes narrow and saturates as 12 μm of optical pitch at higher amplitude. Further increasing the amplitude at low frequencies, the chiral phases slowly melt away and at the same time, the dynamical states of small non-chiral nematic domains appear. The detailed characterizations of kinetics of these dynamical states are done by video correlation functions as discussed in section III.

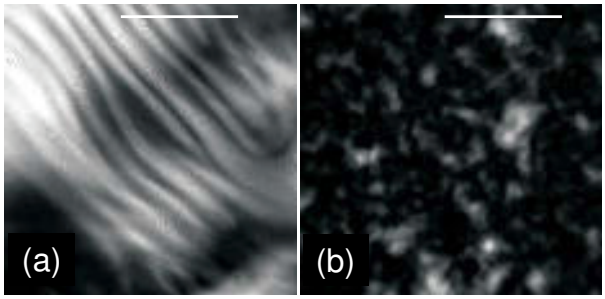

Fig. 2 Depolarized optical morphology at low frequency: (a) chiral-nematic phase, and (b) dynamical states of small non-chiral nematic domain melts and reforms in space and time. The scale bar is approximately 200 um.

B. The Preparation of fd-virus Suspensions

We follow standard biological protocols to prepare the fd-virus suspensions, by using the XL1 blue strain of E-coli host bacteria [6]. The bare length of the fd-virus particles is approximately known as 880 nm, with diameter of 6.7 nm. The surface charge is measured approximately negatively charged as ~ 9000e at pH = 6.9. Molecular level of the understanding of fd-virus particles are provided with NMR studies [8], where the structure and dynamics of fd-coat proteins are shown as slightly "slewed" left-handed alpha-helix form. By changing the ionic strength, the double-layer of diffusive ions are influencing with fd-concentrations. The conductivity is increased with increasing ionic strength; from 791 μS/cm to 12.7 μS/cm, as 20 mM and 0.16 mM ionic strength, respectively. We prepare our fd-suspensions from the dialysis for 2 days against a TRIS/HCl-buffer with an analytical concentration of 1.6 mM ionic strength. Then the fd-concentration is measured by UV spectrometer to read the optical density, or the extinction coefficient at approximately 269 nm wavelength.

C. Vertical Small Angle Dynamic Light Scattering

The simple sketch of our homemade vertical small angle dynamic light scattering is shown in Fig.1 (b). He/Ne laser (~ 633 nm wavelength) is incident from the lower side of the sample that is connected to the function generator. Since this is vertical dynamic light scattering, the bare beam of the incident light should be aligned as a straight-up, within an "accuracy" of 0.01 degree of deviation.

As can be seen in Fig. 1 (b), the detecting side is upper side of the in-situ electric cell equipped with a height-adjustable mount stage. The necessary optical elements are positioned in a single optical rail that combined with motorized rotator. Then it plays as our "goniometry" to collect the scattered laser light from the sample inside bulk. Typical sample thickness is approximately as 1.4 ~ 2.7 mm. To avoid any scattered light coming from near the ITO glass substrates, we particularly include the achromatic lens (~75 mm focal length) above the sample mount.

The enhancement of using this lens is vividly shown in long-time slow relaxation process [4]. Then the signal processing of the resultant microscopic dynamics in increasing field amplitudes are shown in Fig. 3. Intriguingly, a microscopic discontinuity is observed at the transition of chiral-phase and dynamical (in Fig. 3(b)). This is due to the fact of "intrinsic" differences on the microscopic dynamics between chiral-nematic phase and non-chiral nematic domains [3]-[4].

D. Video Correlation Spectroscopy

Time-lapsed images are collected for video correlation spectroscopy. The resolution of the images is small (216 pixel x 170 pixel 8-bit bitmap) for long time duration (~ 1200-1800 s). Time-step is typically chosen from 300 ms to

1 s, depending on the response of system with applying field amplitude at a low frequency. The transmitted intensity of images is converted to readable ASCII format to correlate pixel by pixel intensity averaging at all time-steps. We made a program to calculate the video correlation function, which is discussed in Section III. We have found the best performance of the intensity averaging is 1 pixel by 1 pixel, as compared to 5 pixels by 5 pixels (or 10 pixels by 10 pixels) averaging. This may be related to a low magnification objective lens (10X objective) that is chosen for sampling the larger region of interest (ROI) in the system.

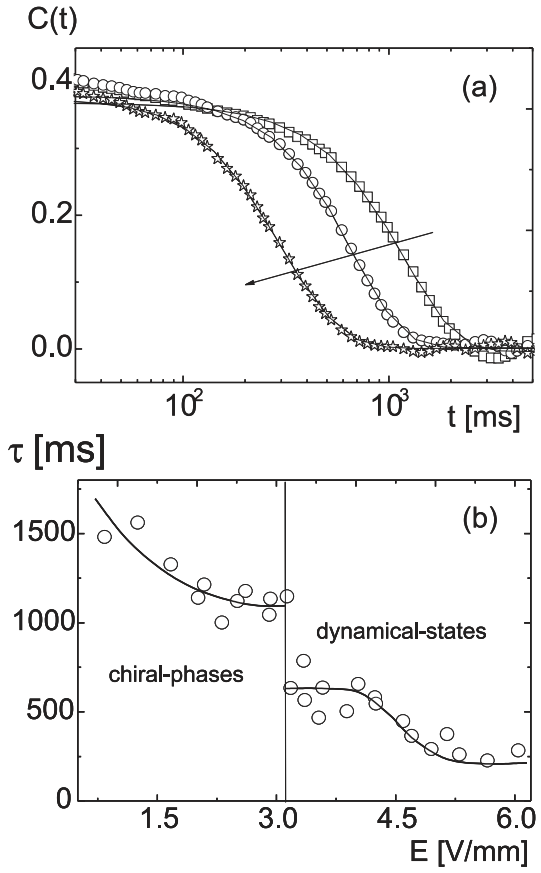

Fig. 3 Vertical dynamic light scattering: (a) typical correlation functions are shown in increasing field amplitude (the arrow indicated). (b) The microscopic relaxation time of fd-virus particles as a function of amplitude of a low frequency.

III. Video Correlation Analysis and Relaxation Time

The relaxation time of the system can be obtained by correlation functions from both signal and image processing, via dynamic light scattering and video correlation spectroscopy, respectively. Fig. 3 (a) have shown typical signal correlations functions of our vertical small angle dynamic light scattering as a function of increasing the field amplitude (as indicated the arrow direction). The relaxation time is decreased as increasing field amplitude (shown in Fig.3 (b)), and the microscopic discontinuity is observed at the transition of chiral-phase to dynamical states (around 3.2 V/mm). At this transition, the chirality slowly disappears and at the same time, non-chiral small nematic domains are becoming dynamic, in terms of their melting and formation of the small non-chiral nematic domains (~ 20 μm).

Above the transition, continuous decrease of the relaxation time is observed in both signal and image processing. For an image processing, we have used the time-lapse video correlation spectroscopy that collects time stacks of region of interests.

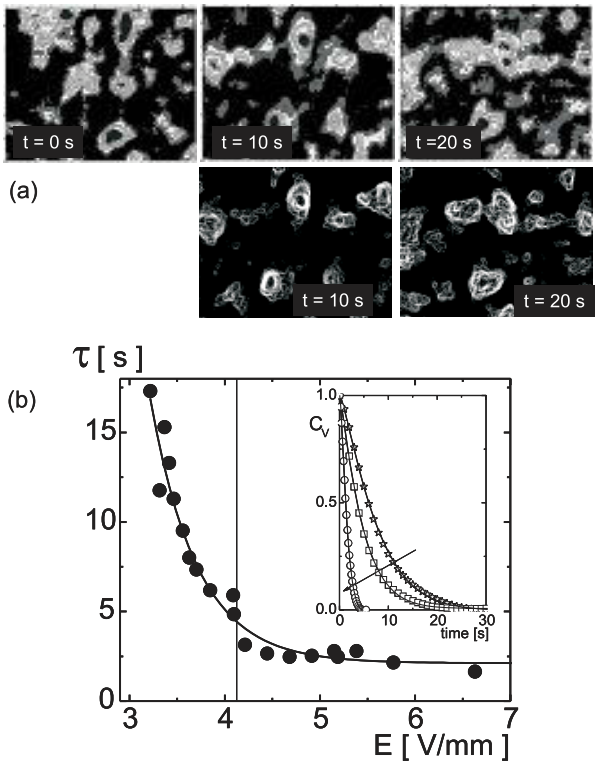

Fig. 4 Video Correlation Analysis: (a) 2D Intensity profiles of raw images at time step as 0 s, 10 s, and 20 s (upper), and the subtracted image of time step for 10 s, and 20 s from the initial image (lower), respectively. (b) The macroscopic relaxation time of dynamical states "fastening" towards higher field amplitude. The insert shows typical video correlation from our analysis, where the arrow indicates increasing field amplitude.

Then the video correlation function is defined as

$$C_V(t) = \frac{\left\langle \left[I(t) - < I(t) > \right] \left[I(0) - < I(0) > \right] \right\rangle}{\left\langle \left[I(0) - < I(0) > \right]^2 \right\rangle}$$

, where I is the transmitted intensity at a given pixel and the brackets <…> denote averaging over all pixels. Typical image speckle patterns of the dynamical states are shown in Fig. 4(a), where the upper images are related to the raw data from at certain time step, and the lower ones are the images of subtracted to the initial intensity profile (at a time t = 0 s).

As one can see, the contrast is enhanced in lower images for taking care of the random positional ensemble sufficiently reduced. Then the correlation functions of the speckles (or our small nematic domains) in time decay as a single stretched exponent, indicated in the insert of Fig. 4(b). Also the time constant for melting and forming as a function of the (higher) field amplitude at a low frequency is shown in Fig. 4(b). Interestingly, the relaxation time diverges on approach from the transition of dynamical states to chiral-phase regime (close to ~ 3.2 V/mm). However the time constant in "fast" dynamical states is essentially independent of the field amplitude at higher field amplitude. This may be related to either the lack of the resolution we may have in our experiments, or the genuine behavior from the system.

IV. Conclusion

The exploration of phase/state transitions in suspensions of charged fibrous viruses (fd) at a low ionic strength has been performed in external electric fields at low frequency, where double-layer is polarized. Particle-particle interactions of fd-virus that is surrounded with thick double-layers are responsible for various chiral-phases and dynamical states through depolarized light that. It is still an open question whether this is due to either the condensed ions against the diffusive ions, or how much contributions from each of them. It would be useful to correlate both image and signal information of fluctuating quantities to extract how the system responses with external fields. We relate our work to enhance the mesoscopic time and length scale imaging correlation of soft-tissues, which is a current challenge to customize the biomedical technology. For had object medical imaging, the density difference can be conveniently "boosted" with the fluorescent dyes for the structural contrast. However, for any soft-organs or tissues that contain fibrous structures, their orientation can be used as "crucial" information within the elastic envelop in biological fluids (or multivalent ionic liquids). ***We have shown that the dynamical situations of soft biological matter (fd-viruses) that responses to the depolarized light as employed by time-lapsed imaging processing.*** It would be desirable in future to make an "integrated" packaging from the time-lapsed imaging processing to pixel-to-pixel intensity auto correlation signal progressing all-in-one.

References

[1] J. Xu, and D. A. Lavan, "Designing artificial cells to harness the biological ion concentration gradient", Nature Nanotechnology, 2008, Advance online publication, doi:10.1038/mnano.2008.274.

[2] C. Tallon-Baudry, and O. Bertrand, "Oscillatory gamma activity in humans and its roles in object representation", Trends in Cognitive Sciences, Vol. 34, No. 4, April 1999, pp. 151-162.

[3] K. Kang, and J. K. G. Dhont, "Double-layer polarization induced transitions in suspensions of colloidal rods", Europhysics. Lett. 84, 2008, pp. 14005-p1 – p6.

[4] K. Kang, and J. K. G. Dhont, "Electric-field induced transitions in suspensions of rods (fd-virus) due to double-layer polarization", submitted for publication.

[5] K. Kang, and J. K. G. Dhont, "Criticality in a non-equilibrium, driven system: Charged colloidal rods (fd-viruses) in electric fields", submitted for publication.

[6] J. Sambrook, E. F. Fritsch, and T. Maniatis, "Molecular cloning: A laboratory manual", in Cold Spring Harbor, New York, 1989.

[7] K. G. Valentine, D. M. Schneider, G. C. Leo, L. A. Colnago, and S. J. Opella, "Structure and dynamics of fd coat protein", Biophys. J., Vol. 49, 1986, pp. 36-38.